Dinitrogen Hapticity

DOI: 10.1002/anie.201301800

Redox-Induced N_2 Hapticity Switching in Zirconocene Dinitrogen Complexes**

*Scott P. Semproni, Donald J. Knobloch, Carsten Milsmann, and Paul J. Chirik**

The functionalization of molecular nitrogen, N_2, using soluble transition-metal complexes has been a long-standing goal in chemical synthesis.[1] At the core of this challenge is understanding the interaction of the N_2 molecule with transition-metal complexes.[2] For metallocenes of the lanthanides[3] and the Group 4 triad,[4,5] side-on coordination of the N_2 ligand has special significance, offering unique electronic structures such as $(N_2)^{3-}$,[6] compounds that act as single molecule magnets,[7] and a wealth of functionalization chemistry, including reactions that couple N≡N cleavage to N–H and N–C bond formation.[8] Although early transition-metal dinitrogen complexes with side-on N_2 coordination are now the most prevalent and dominate the reactivity landscape, this hapticity is by no means a prerequisite for functionalization chemistry. For example, a bis(indenyl)zirconium complex with an activated end-on dinitrogen ligand stabilized by NaCl inclusion undergoes N_2 hydrogenation.[9]

In Group 4 metallocene dinitrogen compounds, controlling N_2 hapticity by manipulation of the steric environment imparted by the cyclopentadienyl substituents is now well-established.[10] For zirconium and hafnium, removing a methyl group from each cyclopentadienyl ring in $[\{(\eta^5\text{-}C_5Me_5)_2M(N_2)\}_2(\mu_2,\eta^1,\eta^1\text{-}N_2)]$ (M = Zr, Hf)[11] induces a change in N_2 hapticity from end-on to side-on.[12] In contrast, for titanium, the smallest metal in the triad, the demarcation occurs when removing a methyl group from $[\{(\eta^5\text{-}C_5Me_4H)_2Ti\}_2(\mu_2,\eta^1,\eta^1\text{-}N_2)]$.[13] Much less is known about the electronic influences on N_2 hapticity in a constant ancillary ligand environment. Herein we describe the synthesis and characterization of *ansa*-zirconocene dinitrogen complexes that reversibly change N_2 hapticity as a function of redox state. The spectroscopic signatures of the anion with end-on N_2 coordination are identical to Lappert's $[(\eta^5\text{-}C_5H_5)_2Zr(R)(\eta^2\text{-}N_2)]$ (R = CH(SiMe$_3$)$_2$),[14] a compound often cited as having the first side-on bound N_2 ligand in a Group 4 metallocene dinitrogen complex. This formulation is also unusual as no monomeric Group 4 metallocene dinitrogen complexes exhibit side-on coordination.[15] Crystallographic and spectroscopic data presented herein revise that structure and provide insight into the fundamental features that govern N_2 hapticity in Group 4 metallocene complexes.

During the course of our continued investigations into structure–reactivity relationships with Group 4 metallocene dinitrogen complexes, a new *ansa*-dicyclopentadienyl ligand, $Li_2[Me_2Si(\eta^5\text{-}C_5Me_4)(\eta^5\text{-}C_5H_3\text{-}3\text{-}^2Ad)]$ (^{2}Ad = 2-adamantyl), and its corresponding zirconium dichloride complex, **1**-Cl_2, were prepared using standard routes.[16] Attempts to synthesize the neutral dinitrogen complex by reduction with 0.5% Na(Hg), the typical procedure to prepare such compounds,[8–12,16] produced an intractable mixture of paramagnetic and diamagnetic zirconium products. By contrast, stirring a diethyl ether–toluene slurry of **1**-Cl_2 with excess KC_8 under an N_2 atmosphere furnished a red crystalline solid identified as the anionic zirconocene dinitrogen complex, K[**1**-N_2]Cl_2, in 51% yield.

X-ray diffraction on red single crystals of K[**1**-N_2]Cl_2 established the molecular structure as the binuclear zirconocene chloride compound with an end-on dinitrogen ligand (Figure 1).[18] A potassium cation, solvated by two equivalents of diethyl ether, interacts with both chloride ions and the N_2 ligand. The zirconocene subunits are arranged such that the bulky 2-adamantyl groups are oriented *anti* across the metallocene wedge. The potassium cation is pseudo symmetrically

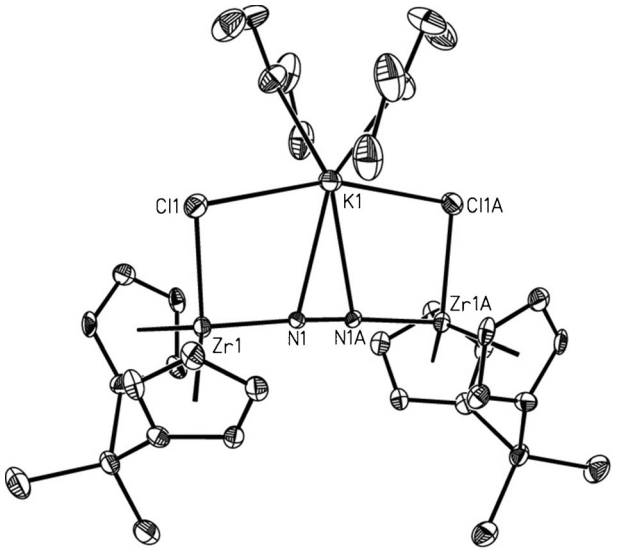

Figure 1. Representation of the solid state structure of K[**1**-N_2]Cl_2 (ellipsoids set at 30% probability). Cyclopentadienyl substituents and hydrogen atoms have been omitted for clarity.

[*] S. P. Semproni, D. J. Knobloch, C. Milsmann, Prof. P. J. Chirik
Department of Chemistry, Princeton University
292 Frick Laboratory, Princeton, NJ 08544 (USA)
E-mail: pchirik@princeton.edu

[**] We thank the Director of the Office of Basic Energy Science, Chemical Sciences Division, U.S. Department of Energy (DE-FG-02-05ER15659) and the ACS Frasch Foundation for financial support. S.P.S. thanks the Natural Sciences and Engineering Research Council of Canada for a predoctoral fellowship and C.M. also acknowledges the Alexander von Humboldt Foundation for a Feodor Lynen postdoctoral fellowship.

Supporting information for this article is available on the WWW under http://dx.doi.org/10.1002/anie.201301800.

disposed between the two zirconocenes. The N–N bond distance of 1.223(9) Å signals modest activation when compared to a related NaCl stabilized bis(indenyl) zirconium complex with an end-on $(N_2)^{4-}$ ligand, which exhibits an N–N bond distance of 1.352(5) Å.[9] By way of calibration, lanthanide dinitrogen complexes with $(N_2)^{3-}$ ligands have N–N distances that range between 1.396(7) and 1.405(3) Å.[6] Therefore, the contracted N–N bond length observed in K[**1**-N_2]Cl_2 is most consistent with values in metallocene dinitrogen complexes assigned as having $(N_2)^{2-}$ ligands.

A solution magnetic moment of 1.6(2) μ_B was measured for the odd-electron *ansa*-zirconocene complex in [D_6]benzene at 23 °C, consistent with one unpaired electron. To gain further insight into the electronic structure of K[**1**-N_2]Cl_2, an EPR spectrum was recorded as a toluene solution at ambient temperature (Figure 2). As part of these studies, the ^{15}N isotopologue, K[**1**-$^{15}N_2$]Cl_2, was prepared by performing the KC_8 reduction of **1**-Cl_2 under an atmosphere of $^{15}N_2$. For the natural-abundance compound, an isotropic signal was observed with $g_{iso} = 2.0028$ and hyperfine coupling ($A_{iso}(^{14}N) = 10.6$ MHz) to two 100 % abundant $I = 1$ nitrogen atoms as well as to ^{91}Zr ($A_{iso}(^{91}Zr) = 17.8$ MHz, $I = 5/2$, 11.2 % abundant). Introduction of $^{15}N_2$ confirmed the coupling to nitrogen as the signal for K[**1**-$^{15}N_2$]Cl_2 collapsed to a triplet ($A_{iso}(^{15}N) = 14.5$ MHz) with additional coupling to ^{91}Zr. Cooling the sample to 100 K (THF glass) produced a broadened rhombic signal ($g_x = 2.021$, $g_y = 1.996$, $g_z = 1.994$) with only resolved ^{14}N hyperfine interactions. No ^{91}Zr hyperfine coupling was observed at this temperature, which was due either to line broadening that occurs upon cooling or spin localization on the bridging N_2 ligand. Cooling the sample to lower temperatures resulted in continued line broadening and generated a featureless spectrum. At 100 K, the A_{iso} value increases to 12.6 MHz (^{14}N), which may be a consequence of greater electron localization on the N_2 ligand. Similar spectroscopic behavior was observed with the ^{15}N isotopologue with appropriate changes in multiplicity resulting from the $I = 1/2$ nuclear spin (Supporting Information, Figure S8).

The oxidation of K[**1**-N_2]Cl_2 was explored with the goal of preparing the neutral dinitrogen complex and establishing its N_2 hapticity and degree of activation. Stirring a toluene solution of K[**1**-N_2]Cl_2 with one equivalent of $AgBPh_4$ cleanly furnished [**1**-N_2]Cl_2 with concomitant precipitation of silver metal and $KBPh_4$. The ^1H NMR spectrum of [**1**-N_2]Cl_2 in [D_6]benzene exhibited the number of resonances consistent with formation of a C_2 symmetric dizirconocene dinitrogen complex. The [D_6]benzene ^{15}N NMR spectrum of the ^{15}N-isotopologue, [**1**-$^{15}N_2$]Cl_2, exhibits a singlet at $\delta = 639.9$ ppm in the range typical of halide-free dinitrogen complexes such as [{(η^5-$C_5Me_4H)_2Zr$}$_2$(μ_2,η^2,η^2-N_2)] ($\delta = 621.1$ ppm).[12a] These data suggest that the substitution of the nitrogen rather than the formal oxidation state of the metal determines the ^{15}N NMR shift. The side-on hapticity of the dinitrogen ligand in [**1**-N_2]Cl_2 was established by X-ray diffraction (Supporting Information, Figure S3). Unfortunately the crystals were weakly diffracting and only molecular connectivity and not metrical parameters could be reliably established. We note that the Zr–Zr distance of 4.370(4) Å is as expected for a zirconocene complex with a side-on dinitrogen ligand.[12]

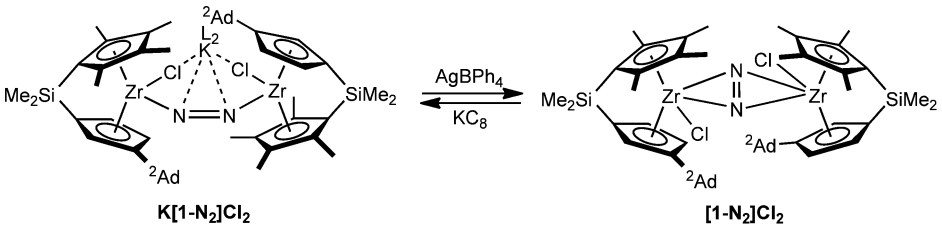

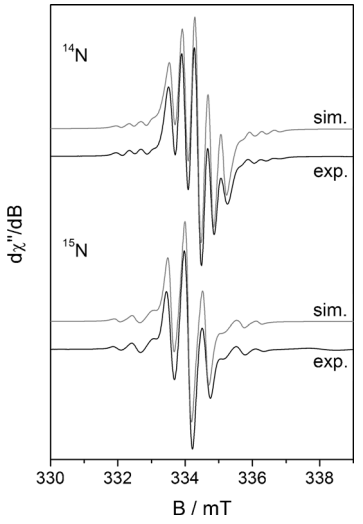

Figure 2. Experimental (black) and simulated (gray) X-band EPR spectrum of K[**1**-N_2]Cl_2 (top) and K[**1**-$^{15}N_2$]Cl_2 (bottom) collected in toluene at 295 K. Simulated parameters: $g_{iso} = 2.0028$, $A_{iso}(^{14}N) = 10.6$ MHz, $A_{iso}(^{15}N) = 14.5$ MHz, $A_{iso}(^{91}Zr)$: 17.8 MHz (assuming 11.22 % naturally occurring ^{91}Zr with $I = 5/2$).

The electronic structures of K[**1**-N_2]Cl_2 and [**1**-N_2]Cl_2 were also investigated with DFT calculations. The HOMO of the neutral, *ansa*-zirconocene dinitrogen complex, [**1**-N_2]Cl_2, is presented in Figure 3 and is best described as a π-backbond from a linear combination of zirconocene b_2 orbitals with the in-wedge N_2 π* orbitals similar to the electronic structure reported for [{Me_2Si(η^5-C_5Me_4)(η^5-C_5H_3-3-*t*Bu)ZrH}$_2$(μ_2,η^2,η^2-N_2)].[16] The LUMO is comprised of N_2 π* orbitals of δ symmetry, which owing to the presence of the chloride ligand do not have an appropriate metal orbital with which to overlap. In cases where the additional X-ligand is absent in the wedge, such as [{(η^5-$C_5Me_4H)_2Zr$}$_2$(μ_2,η^2,η^2-N_2)], an out-of-phase combination of $1a_1$ zirconocene orbitals interacts with the δ symmetry N_2 π* and is responsible for the formation of the $(N_2)^{4-}$ ligand.[12b] One-electron reduction and alkali metal coordination induces a change in N_2 hapticity from side-on to end-on and changes the frontier molecular orbital picture. The DFT computed SOMO and SOMO−1 (Figure 3) are each comprised of linear combinations of zirconocene b_2 orbitals interacting with the perpendicular π* molecular orbitals of the end-on dinitrogen ligand. The DFT

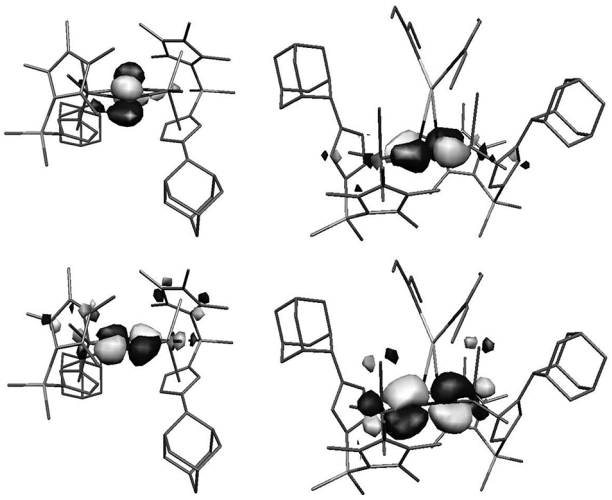

Figure 3. DFT-computed LUMO and HOMO (top and bottom, left) of [**1**-N_2]Cl_2 and SOMO and SOMO−1 (top and bottom, right) of K[**1**-N_2]Cl_2.

computed N−N bond distance in [**1**-N_2]Cl_2 of 1.227 Å is indistinguishable from the experimental value of 1.223(9) Å measured in K[**1**-N_2]Cl_2 (DFT(N−N) = 1.235 Å), suggesting that the population of the molecular orbitals perpendicular to the metallocene wedge offers little in the way of dinitrogen reduction.

As shown in Figure 4, the DFT computed spin density is consistent with observations from ambient temperature EPR spectroscopy. The unpaired spin is delocalized over the

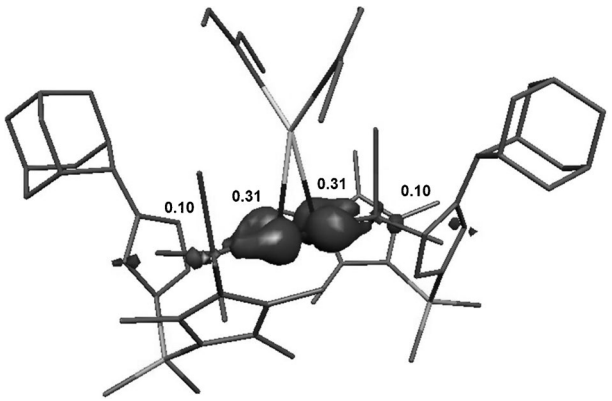

Figure 4. DFT-computed spin density plot for K[**1**-N_2]Cl_2 from Mulliken population analysis. For a color version, see the Supporting Information, Figure S17.

{Zr_2N_2} core with the majority of the spin residing on the dinitrogen ligand. Thus, the overall electronic structure of K[**1**-N_2]Cl_2 is best described as a hybrid of Zr^{IV}–$(N_2)^{3-}$–Zr^{IV} and Zr^{III}–$(N_2)^{-}$–Zr^{III}. The experimentally determined N–N distance of 1.223(9) Å is consistent with this view of the bonding in the molecule.

The reversibility of the redox-induced hapticity change was explored by both electrochemical and chemical methods. The cyclic voltammogram (Supporting Information, Figure S22) in THF exhibited multiple irreversible oxidation and reduction waves independent of scan rate. The association/dissociation of the potassium cation with the N_2 ligand that accompanies the redox-induced hapticity change is believed to be the origin of this behavior (see below). Electron transfer between K[**1**-N_2]Cl_2 and [**1**-N_2]Cl_2 was explored by NMR and EPR spectroscopies in THF solution and glass. No change in the features of the spectra was observed upon mixing the compounds suggesting that intermolecular electron transfer does not occur on the timescale of either technique. The redox-induced hapticity switching did however prove chemically reversible, as treatment of the neutral compound [**1**-N_2]Cl_2 with KC_8 furnished K[**1**-N_2]Cl_2, and oxidation of K[**1**-N_2]Cl_2 with $AgBPh_4$ yielded [**1**-N_2]Cl_2. While pure products were obtained in each step because of differential solubility, each synthetic transformation produced only 50% yield of isolated product. Thus, the sequence was only repeated for a few cycles owing to the material losses associated with each step.

The EPR spectrum of K[**1**-N_2]Cl_2 was reminiscent of data published by Lappert and co-workers for the zirconocene alkyl complex with a purported side-on dinitrogen ligand, [(η^5-C_5H_5)$_2$Zr(R)(η^2-N_2)].[14] Because K[**1**-N_2]Cl_2 contained an end-on dinitrogen ligand stabilized by alkali metal coordination, we sought to reconcile the apparent difference between the two compounds by preparing and structurally characterizing Lappert's example. Following the published procedure,[14] yellow-brown plates suitable for X-ray diffraction were obtained and a representation of the molecular structure is presented in Figure 5.[18] The crystallographic data definitively establish an anionic, bimetallic rather than

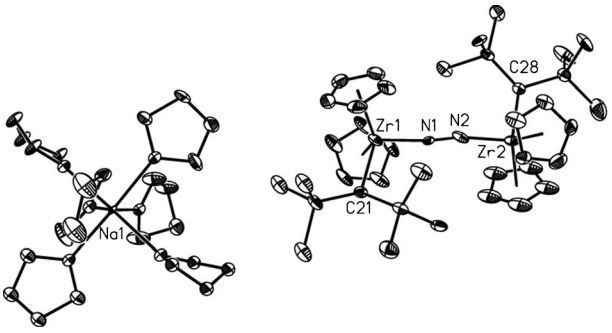

Figure 5. ORTEP of [Na(thf)$_6$][**2**-N_2] (ellipsoids set at 30% probability). Hydrogen atoms and disordered orientations of THF solvate have been omitted for clarity.

monomeric alkyl zirconocene compound with a bridging, end-on coordinated dinitrogen ligand and a sodium cation. Unlike the potassium cation in K[**1**-N_2]Cl_2, the sodium ion in [Na(thf)$_6$][**2**-N_2] exhibits no close contacts with the dizirconocene anion. The N–N bond distance of 1.228(9) Å signals modest activation and is indistinguishable from the value in K[**1**-N_2]Cl_2. As in K[**1**-N_2]Cl_2, the extremely sterically demanding $CH(SiMe_3)_2$ groups are positioned *anti* to one another across the dimer and effectively block both sides of the anion and likely discourage interaction of the cation with the bridging dinitrogen ligand. The structural data on both

$[Na(thf)_6][\mathbf{2}\text{-}N_2]$ and $K[\mathbf{1}\text{-}N_2]Cl_2$ establish the preference for end-on coordination in anionic dinitrogen complexes.

To confirm that the crystallographic data on $[Na(thf)_6][\mathbf{2}\text{-}N_2]$ were indeed representative of the bulk sample and identical to the material isolated by Lappert, EPR data were obtained. The ambient temperature EPR spectra of $[Na(thf)_6][\mathbf{2}\text{-}N_2]$ and the ^{15}N isotopologue, $[Na(thf)_6][\mathbf{2}\text{-}^{15}N_2]$, were recorded in THF solution and are presented in the Supporting Information, Figure S6. Comparison of the spectra establish that the two compounds exhibit virtually identical spectroscopic signatures and are in agreement with those originally reported by Lappert.[14] Thus, $[Na(thf)_6][\mathbf{2}\text{-}N_2]$ is an anionic zirconium dinitrogen complex with a modestly activated, end-on N_2 ligand. Importantly, EPR spectroscopy has proven to be a powerful technique for identification of this new class of anionic zirconocene dinitrogen complex. The structural revision of $[Na(thf)_6][\mathbf{2}\text{-}N_2]$ renders Fryzuk's $[\{[(i\mathrm{Pr}_2\mathrm{PCH}_2\mathrm{SiMe}_2)_2\mathrm{N}]\mathrm{ZrCl}\}_2(\mu_2,\eta^2,\eta^2\text{-}N_2)]$ the first example of side-on dinitrogen coordination with a Group 4 transition-metal complex.[17]

Because of the hapticity change induced by oxidation of $K[\mathbf{1}\text{-}N_2]Cl_2$, the neutral variant of Lappert's dinitrogen compound, reported as $[\{(\eta^5\text{-}C_5H_5)_2Zr(R)\}_2(\mu_2,\eta^1,\eta^1\text{-}N_2)]$ ($\mathbf{2}\text{-}N_2$), was also prepared and crystallographically characterized. A representation of the molecular structure is reported in the

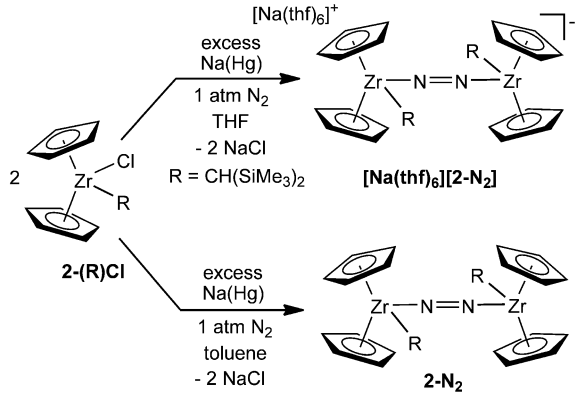

Supporting Information, Figure S4 and confirms retention of the end-on hapticity of the dinitrogen ligand. The N–N bond distance of 1.175(4) Å is contracted from the corresponding anion. As with $[Na(thf)_6][\mathbf{2}\text{-}N_2]$, the large alkyl groups are in an *anti* disposition across the zirconium dimer. The dihedral angles of the metallocene wedges in $\mathbf{2}\text{-}N_2$ are equivalent by symmetry and are equal to 168.9(14)°. By comparison, the dihedral angles in $[Na(thf)_6][\mathbf{2}\text{-}N_2]$, are 159(3)° and 157(2)°, indicating only a minor geometric reorganization occurs upon formation of the anion again consistent with the alkyl ligands dictating the overall molecular geometry. It is likely that the spectator anionic ligand in the metallocene wedge, for example, chloride and $[CH(SiMe_3)_2]$, rather than cyclopentadienyl substitution, determines N_2 hapticity.

The cyclic voltammogram of $[Na(thf)_6][\mathbf{2}\text{-}N_2]$ in THF (Supporting Information, Figure S21) exhibits two reversible anodic waves, consistent with oxidation to the neutral compound, and an as-yet unobserved monocationic zirconocene species. This behavior contrasts the irreversible electrochemistry observed with the *ansa*-zirconocene compound and is most likely due to the retention in N_2 hapticity and lack of alkali metal dissociation–coordination associated with the redox events. Accordingly, intermolecular electron transfer occurs on the NMR timescale as evidenced by broadening of the $[D_6]$benzene solution ^1H resonances for diamagnetic $\mathbf{2}\text{-}N_2$ upon addition of sub-stoichiometric quantities of $[Na(thf)_6][\mathbf{2}\text{-}N_2]$. We note that addition of the paramagnetic titanocene complex with a side-on coordinated N_2 ligand, $[\{(\eta^5\text{-}C_5H_2\text{-}1,2,4\text{-}Me_3)_2Ti\}_2(\mu_2,\eta^1,\eta^1\text{-}N_2)]$,[13b] had no effect on the $[D_6]$benzene NMR spectrum of $\mathbf{2}\text{-}N_2$. These results demonstrate that the absence of a gross structural change arising from N_2 hapticity switching and alkali metal coordination that accompany oxidation and reduction results in more facile intermolecular electron transfer.

A DFT computational study was also conducted on the neutral and anionic compounds, $\mathbf{2}\text{-}N_2$ and $[Na(thf)_6][\mathbf{2}\text{-}N_2]$, respectively. The dinitrogen ligand retains its N_2 hapticity upon reduction and the electronic structure is not complicated by interaction of the sodium cation with the dinitrogen ligand. As shown in the Supporting Information, Figure S16, the HOMO of $\mathbf{2}\text{-}N_2$ is a linear combination of in-wedge zirconocene N_2 π^* orbitals likely responsible for the observed N–N elongation. The DFT computed N–N bond distance of 1.179 Å is excellent agreement with the crystallographic distance of 1.175(4) Å. One-electron reduction to $[Na(thf)_6][\mathbf{2}\text{-}N_2]$ generates a SOMO comprised of molecular orbitals of b_2 symmetry perpendicular to the metallocene wedge. As with $K[\mathbf{1}\text{-}N_2]Cl_2$, population of this orbital results in a slight elongation of the N_2 ligand as the N–N bond distance in $[Na(thf)_6][\mathbf{2}\text{-}N_2]$ of 1.228(9) Å is only slightly elongated from the neutral compound. The combination of EPR spectroscopic data and computed spin density (Supporting Information, Figure S18) establish a similar electronic structure to $K[\mathbf{1}\text{-}N_2]Cl_2$. Thus, the N_2 ligand in $[Na(thf)_6][\mathbf{2}\text{-}N_2]$ is best described as a hybrid between $(N_2)^{3-}$ and $(N_2)^{-}$, consistent with the experimentally determined N–N bond distance of 1.228(9) Å.

In summary, oxidation and reduction has been established as a method for inducing reversible changes in N_2 hapticity in an *ansa*-zirconocene complex. The associated structural reorganization and alkali metal coordination–dissocation increases the barrier for intermolecular electron transfer between neutral and anionic compounds. In the parent zirconocene example, end-on hapticity is retained upon oxidation and reduction enabling facile electron transfer between neutral and anionic complexes. Both formally anionic zirconocene dinitrogen complexes contain rare examples of N_2 ligands best described as a hybrid between $(N_2)^{3-}$ and $(N_2)^{-}$. The odd-electron character associated with this unusual N_2 electronic structure may translate into functionalization reactivity unique from previously established neutral and radical methods reported for side-on bound N_2 fragments and is an avenue currently under investigation.

Received: March 2, 2013
Published online: April 15, 2013

Keywords: EPR spectroscopy · dinitrogen ligands · hapticity · redox switch · zirconium

[1] M. Mori, *J. Organomet. Chem.* **2004**, *689*, 4210.
[2] P. L. Holland, *Dalton Trans.* **2010**, *39*, 5415.
[3] a) W. J. Evans, T. A. Ulibarri, J. W. Ziller, *J. Am. Chem. Soc.* **1988**, *110*, 6877; b) W. J. Evans, N. T. Allen, J. W. Ziller, *J. Am. Chem. Soc.* **2001**, *123*, 7927; c) N. T. Allen, J. W. Ziller, *Angew. Chem.* **2002**, *114*, 369; *Angew. Chem. Int. Ed.* **2002**, *41*, 359.
[4] E. A. MacLachlan, M. D. Fryzuk, *Organometallics* **2006**, *25*, 1530.
[5] P. J. Chirik, *Dalton Trans.* **2007**, 16.
[6] a) W. J. Evans, M. Fang, G. Zucchi, F. Furche, J. W. Ziller, R. M. Hoekstra, J. I. Zink, *J. Am. Chem. Soc.* **2009**, *131*, 11195; b) P. J. Chirik, *Nat. Chem.* **2009**, *1*, 520; c) M. Fang, J. E. Bates, S. E. Lorenz, D. S. Lee, D. B. Rego, J. W. Ziller, F. Furche, W. J. Evans, *Inorg. Chem.* **2011**, *50*, 1459.
[7] a) J. D. Rinehart, M. Fang, W. J. Evans, J. R. Long, *Nat. Chem.* **2011**, *3*, 538; b) J. D. Rinehart, M. Fang, W. J. Evans, J. R. Long, *J. Am. Chem. Soc.* **2011**, *133*, 14236.
[8] a) S. P. Semproni, C. Milsmann, P. J. Chirik, *Angew. Chem.* **2012**, *124*, 5303; *Angew. Chem. Int. Ed.* **2012**, *51*, 5213; b) D. J. Knobloch, S. P. Semproni, E. Lobkovsky, P. J. Chirik, *J. Am. Chem. Soc.* **2012**, *134*, 3377; c) S. P. Semproni, E. Lobkovsky, P. J. Chirik, *J. Am. Chem. Soc.* **2011**, *133*, 10406; d) D. J. Knobloch, E. Lobkovsky, P. J. Chirik, *J. Am. Chem. Soc.* **2010**, *132*, 15340; e) D. J. Knobloch, E. Lobkovsky, P. J. Chirik, *J. Am. Chem. Soc.* **2010**, *132*, 10553; f) D. J. Knobloch, E. Lobkovsky, P. J. Chirik, *Nat. Chem.* **2010**, *2*, 30.
[9] D. Pun, C. A. Bradley, E. Lobkovsky, I. Keresztes, P. J. Chirik, *J. Am. Chem. Soc.* **2008**, *130*, 14046.
[10] J. A. Pool, P. J. Chirik, *Can. J. Chem.* **2005**, *83*, 286.
[11] a) J. M. Manriquez, J. E. Bercaw, *J. Am. Chem. Soc.* **1974**, *96*, 6229; b) D. M. Roddick, M. D. Fryzuk, P. F. Siedler, G. L. Hillhouse, J. E. Bercaw, *Organometallics* **1985**, *4*, 97.
[12] a) J. A. Pool, E. Lobkovsky, P. J. Chirik, *Nature* **2004**, *427*, 527; b) J. A. Pool, W. H. Bernskoetter, P. J. Chirik, *J. Am. Chem. Soc.* **2004**, *126*, 14326; c) W. H. Bernskoetter, A. V. Olmos, E. Lobkovsky, P. J. Chirik, *Organometallics* **2006**, *25*, 1021.
[13] a) J. M. de Wolf, R. Blaauw, A. Meetsma, J. H. Teuben, R. Gyepes, V. Varga, K. Mach, N. Veldman, A. L. Spek, *Organometallics* **1996**, *15*, 4977; b) T. E. Hanna, W. H. Bernskoetter, M. W. Bouwkamp, E. Lokbovsky, P. J. Chirik, *Organometallics* **2007**, *26*, 2431; c) S. P. Semproni, C. Milsmann, P. J. Chirik, *Organometallics* **2012**, *31*, 3672.
[14] a) M. J. S. Gynane, J. Jeffrey, M. F. Lappert, *J. Chem. Soc. Chem. Commun.* **1978**, 34; b) J. Jeffrey, M. F. Lappert, P. I. Riley, *J. Organomet. Chem.* **1979**, *181*, 25.
[15] T. E. Hanna, E. Lobkovsky, P. J. Chirik, *J. Am. Chem. Soc.* **2006**, *128*, 6018.
[16] T. E. Hanna, I. Keresztes, E. Lobkovsky, P. J. Chirik, *Inorg. Chem.* **2007**, *46*, 1675.
[17] M. D. Fryzuk, T. S. Haddad, S. J. Rettig, *J. Am. Chem. Soc.* **1990**, *112*, 8185.
[18] CCDC 917112 K[**1**-N_2]Cl_2, 917113 [K([18]crown-6)][**1**-Cl_2], 917114 [Na(thf)$_6$][**2**-N_2], and 917115 [**2**-N_2] contain the supplementary crystallographic data for this paper. These data can be obtained free of charge from The Cambridge Crystallographic Data Centre via www.ccdc.cam.ac.uk/data_request/cif.

